Synthesis of non-symmetric *N*-benzylbispidinol amides and study of their inhibitory activity against the main protease of the SARS-CoV-2 virus

*A. I. Dalinger,[a] D. S. Baev,[b] O. I. Yarovaya,[b] V. Yu. Chirkova,[c] E. A. Sharlaeva,[c] S. V. Belenkaya,[d,e] D. N. Shcherbakov,[c,e] N. F. Salakhutdinov,[b] and S. Z. Vatsadze[f]***

[a]*Lomonosov Moscow State University, Build. 3, 1 Leninskie Gory, 119991 Moscow, Russian Federation*
[b]*N. N. Vorozhtsov Novosibirsk Institute of Organic Chemistry, Siberian Branch of the Russian Academy of Sciences, 9 prosp. Acad. Lavrentieva, 630090 Novosibirsk, Russian Federation*
[c]*Altai State University, 61 prosp. Lenina, 656049 Barnaul, Russian Federation*
[d]*Novosibirsk State University, 2 ul. Pirogova, 630090 Novosibirsk, Russian Federation*
[e]*State Research Center of Virology and Biotechnology VECTOR, Federal Service for Surveillance on Consumer Rights Protection and Human Wellbeing, 630559 Koltsovo, Novosibirsk region, Russian Federation*
[f]*N. D. Zelinsky Institute of Organic Chemistry, Russian Academy of Sciences, 47 Leninsky prosp., 119991 Moscow, Russian Federation. E-mail: vatsadze@ioc.ac.ru*

Based on the data obtained by molecular modeling of the non-covalent interaction of non-symmetric *N*-benzylbispidin-9-ol amides with the active site of the main protease 3CLpro of the SARS-CoV-2 virus, a series of compounds was synthesized, and their inhibitory activity against 3CLpro was studied and compared with that of the known inhibitor ML188 (IC_{50} = 1.56±0.55 μmol L^{-1}). It was found that only compound **1g** containing the 1,4-dihydroindeno[1,2-*c*]pyrazole fragment showed moderate activity (IC_{50} = 100±5.7 μmol L^{-1}) and was characterized by the highest calculated binding energy among the studied bispidine derivatives according to molecular docking data.

Key words: bispidine, SARS-CoV-2, inhibition, main viral protease, 3CLpro, molecular docking, amides.

3,7-Diazabicyclo[3.3.1]nonane (bispidine) belongs to the so-called "privileged scaffolds" in medicinal chemistry,[1] which is explained by the wide range of biological activity exhibited by compounds based on it. The key features of the bispidine framework, which allow it to be widely used in medicinal

* Vatsadze Sergey Zurabovich, born in 1967, Doctor of Chemical Sciences, Professor of the Russian Academy of Sciences, head of the laboratory of the N. D. Zelinsky Institute of Organic Chemistry of the Russian Academy of Sciences, candidate for corresponding member of the Russian Academy of Sciences in the elections in 2022, specialist in organic, supramolecular, and coordination chemistry, co-author of 162 scientific papers, 1 monograph and 6 patents. In his works the application of supramolecular approaches in organic chemistry, medicinal chemistry, and organic materials science have been developed, the design, synthesis, and properties of new molecules as components of functional supramolecular ensembles and materials based on them have been considered. He developed methods for the synthesis of polydentate polyheterocyclic compounds, synthesized luminescent biotags and materials for OLEDs based on substituted pyrazolecarboxylic acids, studied in detail the interactions of original compounds with the main SARS-CoV-2 viral protease using experimental and theoretical methods, revealed new promising representatives of supramolecular and coordination polymers, and developed new catalysts based on conjugates of bispidines and natural chiral terpenes. S. Z. Vatsadze teaches at the Higher Chemical College of the Russian Academy of Sciences, since 2012 he has taught courses on modern organic chemistry created by him for postgraduate students of the Division of Organic Chemistry of Moscow State University. Under his leadership, 6 candidate dissertations were prepared. S. Z. Vatsadze is executive secretary of the editorial board of the *Russian Chemical Bulletin*, member of dissertation councils of Peoples´ Friendship University of Russia, Lomonosov Moscow State University, D. Mendeleev University of Chemical Technology of Russia.

Published in Russian in *Izvestiya Akademii Nauk. Seriya Khimicheskaya,* Vol. 72, No. 1, pp. 239—247, January, 2023.
1066-5285/23/7201-0239

chemistry and pharmacology, are the possibility of selective functionalization of both nitrogen atoms of bispidine,[2–4] the controlled conformational behavior of its bicyclic framework,[5] and pronounced capability to complexation.[6,7] In particular, bispidine derivatives were investigated as potential inhibitors of serine proteases, including thrombin and factor Xa,[8,9] as well as inhibitors of Japanese encephalitis virus.[10]

We showed previously[11] that symmetric *N*,*N*′-disubstituted derivatives of 3,7-diazobicyclo[3.3.1]nonane containing a carboxyl group at position 9 of the bicycle exhibit high inhibitory activity against the main 3CLpro protease of the SARS-CoV-2 coronavirus. The present study continues our investigations aimed at the search for highly efficient inhibitors of the main protease of SARS-CoV-2. Taking into account the known data on the biological activity of *N*-benzylbispidin-9-ols[8] and the high inhibitory activity of symmetric *N*,*N*′-diamides of bispidine,[11] in this work, we synthesized a series of non-symmetric *N*-benzylbispidin-9-ol amides with different amide groups and studied their biological activity.

Results and Discussion

The following principles were used when *N*-benzylbispidinol amides **1a—j** were designed: 1) the carbonyl group at position 9 of the bicycle was replaced with a hydroxyl group to prevent covalent binding with the enzyme; 2) the *N*-benzyl substituent at one nitrogen atom was present in all compounds since *N*,*N*′-dibenzylbispidine was one of the most active compounds in the series of symmetric derivatives; [11] 3) substituents in the amide fragment at the second nitrogen atom were varied. It should be noted that the choice of the latter substituents was based both on the previous experimental data and on the new data of computer modelling.

Synthesis of target compounds. Formyl derivative **1a** was obtained in 64% yield by benzylation of 5,7-dimethyl-1,3-diazaadamantan-6-one and subsequent opening of the diazaadamantane cycle in the presence of KOH (5 equiv.), which was accompanied by the ketone group reduction (Scheme 1).[12]

Amides **1b—h** were obtained in yields from 58 to 86% by acylation of *N*-benzyl-1,5-dimethylbispidin-9-ol (**2**) with equimolar amounts of corresponding acyl chlorides **3** in acetonitrile in the presence of triethylamine as a base at room temperature (Scheme 2).

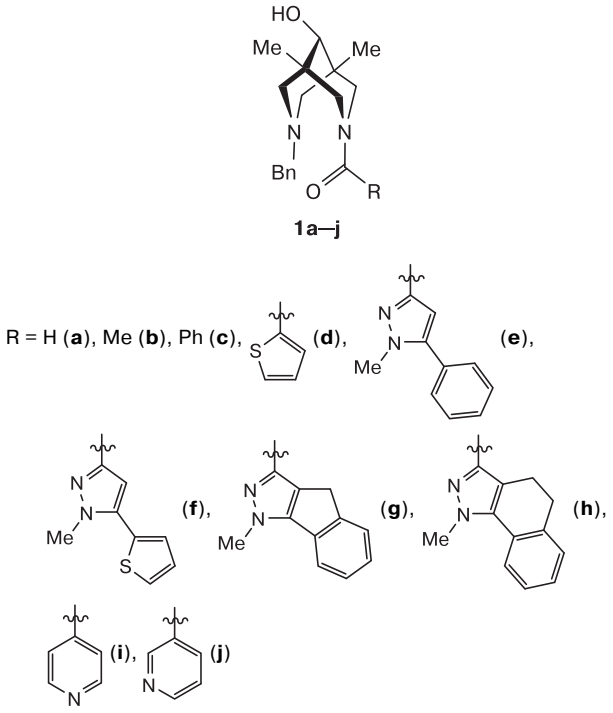

Scheme 1

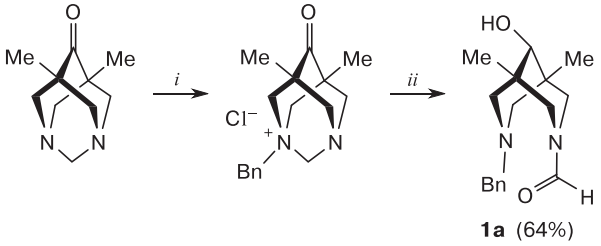

Reagents and conditions: *i*. BnCl, C_6H_6, Δ, 6 h; *ii*. KOH (5 equiv.), H_2O, ~ 20 °C, 12 h.

Scheme 2

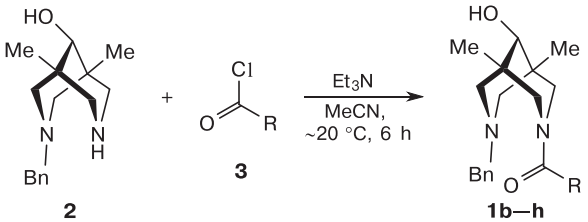

Compound **1**	Yield (%)	Compound **1**	Yield (%)
b	58	**f**	86
c	69	**g**	76
d	66	**h**	80
e	80		

Amides **1i** and **1j** were prepared in the 50 and 54% yields by acylation of *N*-benzyl-1,5-dimethylbispid-

in-9-ol (**2**) with hydrochlorides of isonicotinoyl and nicotinoyl chlorides, respectively, in the presence of triethylamine (2 equiv.) in acetonitrile at room temperature (Scheme 3).

Scheme 3

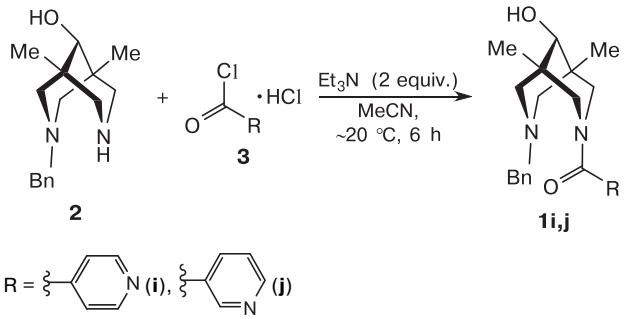

All synthesized compounds were fully characterized by modern physicochemical methods of analysis such as ^{1}H and ^{13}C NMR spectroscopy and high resolution mass spectrometry.

Molecular modelling. Currently, a large number of chemical compounds have been found that can inhibit the activity of the main protease of SARS-CoV-2 due to non-covalent interactions with the amino acids of the active center of the enzyme.[13—17] The search for non-covalent inhibitors based on the bispidine platform significantly expands the knowledge about their possible antiviral effect. Because the replacement of the carbonyl group at position 9 of the bicycle with a hydroxyl group was performed in order to prevent covalent binding to the enzyme, our efforts were directed to modeling the possible non-covalent interactions of new derivatives with the active site of the main protease of SARS-CoV-2. Both the estimated energy of interactions in the ligand—receptor complex and the formation of non-covalent bonds between the atoms of the new derivatives and the catalytic amino acid residue Cys145, as well as the amino acid residue His41 involved in the catalytic process were taken into account.

As a result of the evaluation of the molecular docking, the minimum binding energy values (*E*) shown in Fig. 1 were obtained.

On the whole, compounds **1a—j** exhibit higher binding energy (lower affinity) with the active center of the main protease of SARS-CoV-2 as compared to the ML188 inhibitor. According to the data of the authors of the X-ray diffraction model of the non-covalent interactions between the ML188 inhibitor

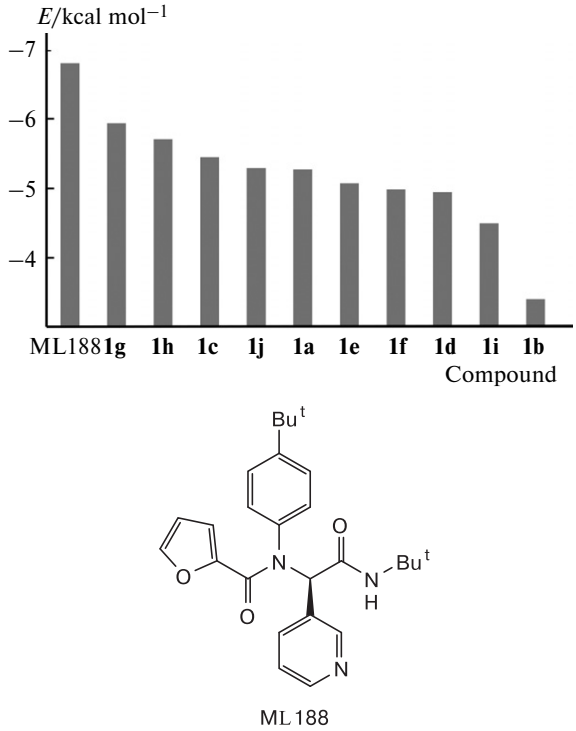

Fig. 1. The results of the estimated function of docking in comparison with the co-crystallized inhibitor ML188 (the minimum binding energy *E* is not true energy, it is considered as an estimated value).

and the main protease of SARS-CoV-2, the inhibitory activity is associated with the stabilization of the flexible loop structures of the main protease active site in the 141—145 chain region and with the non-covalent interactions with the amino acid residues Cys145 and His41, which perform the catalytic function of the enzyme.[16] A branched molecular structure of the ML188 inhibitor readily occupies pockets of the active center of the main protease, realizing a series of non-covalent interactions with amino acids in the 141—145 chain region due to the acceptor oxygen atoms of its furan ring and due to its amide group, as well as due to the π-system of its pyridine ring. The catalytically active amino acid residue Cys145 binds to the π-system of the furan cycle of the inhibitor through non-covalent interactions with the cysteine sulfur atom. The stacking interaction between the phenyl ring of the inhibitor and the His41 imidazole ring provides additional stabilization of the inhibitor in the active site, preventing the catalytic function of the enzyme. Further stabilization of the ML188 conformation in the active center of the main protease is provided by the interactions with Met49, His163, and Glu166 (Fig. 2, *a*).

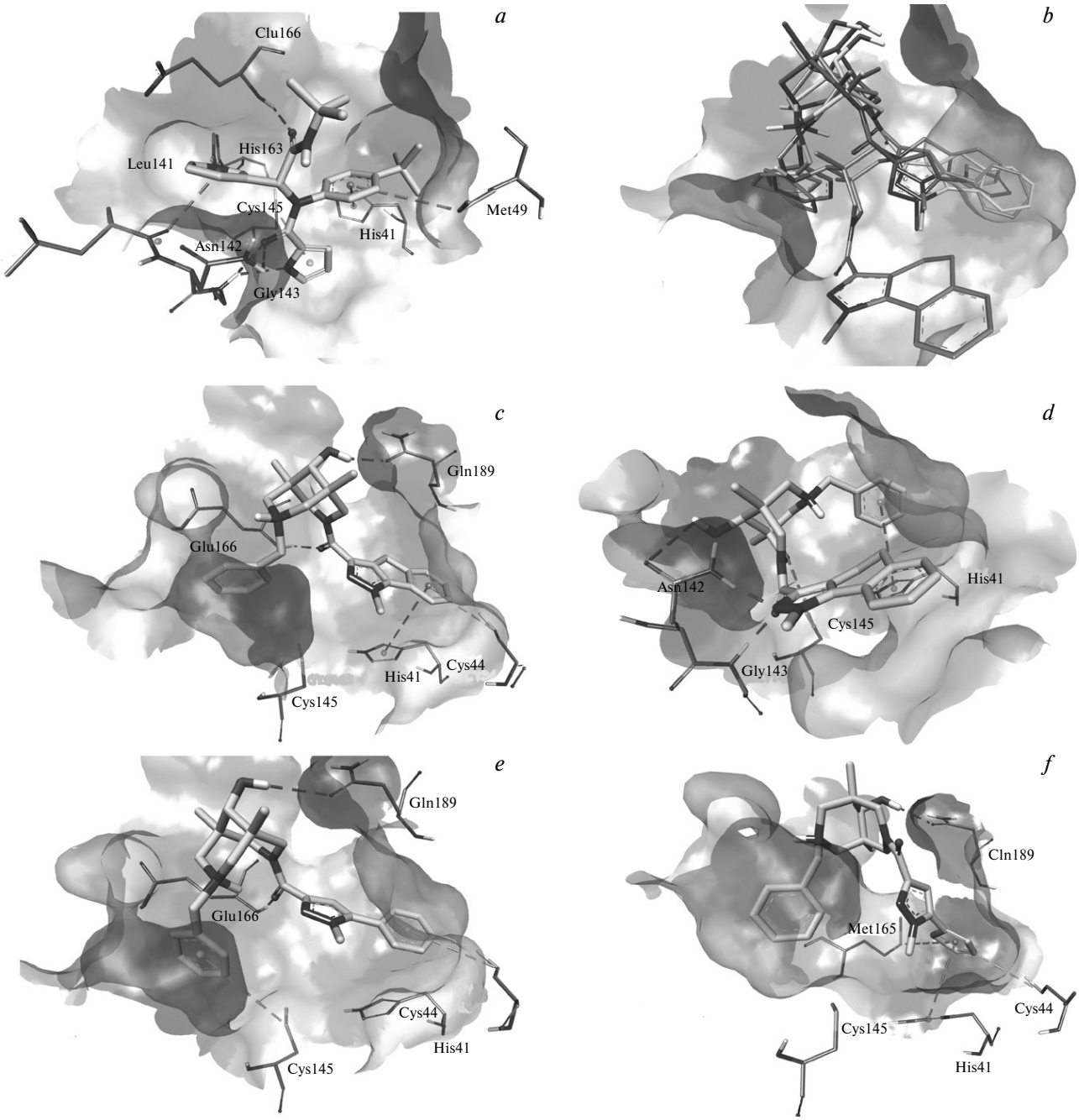

Fig. 2. Specific features of the location of new bispidine derivatives and the ML188 inhibitor in the active site of the main protease of SARS-CoV-2 (non-covalent interactions between the compounds and the active site are shown by dashed lines): ML188 (*a*), superposition of structures **1e—h** (**1g** is yellow, **1h** is green, **1e** is orange, **1f** is blue) in the active site (*b*), **1g** (*c*), **1h** (*d*), **1e** (*e*), **1f** (*f*).

Among the new bispidine derivatives, a group of compounds (**1e**—**g**) stands out. They have uniform arrangement in the active site of the main protease of SARS-CoV-2 (Fig. 2, *b*, *c*, *e*, *f*). Their bulky hydrophobic bispidine framework is located in the space occupied by the *tert*-butylamino group of the ML188 inhibitor, while their unsymmetrical side substituents are located in the regions of the active site, where the ML188 pyridine ring and its *tert*-butylphenyl group are located. This arrangement of these derivatives makes it possible to mimic three of four pharmacophoric groups of ML188. Apparently, this conformation of the bispidine derivatives is best suited for the occupation of a majority of pockets of the active site.

It is interesting to note that compound **1h** (Fig. 2, *d*) having a slightly bulkier side substituent than compound **1g** because of the presence of the intermediate six-membered ring is unable to occupy the same position in the active site of the main protease, which results in the displacement of its bispidine framework towards the center of the active site. Conformations of compounds **1e** and **1f** differ minimally, as well as their estimated binding energies.

The majority of the new bispidine derivatives (**1b,c,f—j**) are capable of stacking interactions with the aromatic system of the amino acid residue His41 due to the π-system of one of side substituents. The strong non-covalent interaction with the Cys145 amino acid residue is characteristic of compounds **1c** and **1e** only; in this case, the sulfur atom of the SH group of Cys145 interacts with the π-systems of side substituents of these derivatives. Lake in the case of the ML188 inhibitor, additional stabilizing hydrogen bonds are formed by compounds **1a—c,e,g,i** with the Glu166 amino acid residue. Possibly, compounds **1d** and **1h** can interact with amino acid residues of the 141—145 chain region due to the correspondence of their molecular structures to this region, which, however, distances them from the amino acid residue Glu166. A specific feature of bispidine derivatives, which differs them from the ML188 inhibitor, consists in their interactions with amino acid residues Gln189 and Cys44.

Biological testing. In order to verify the predicted biological activity, all compounds **1a—j** were tested for the ability to inhibit the main viral protease 3CLpro using a method previously developed by us.[11] The method consists in the measure of the fluorescence level of a peptide substrate interacting with the sensitive 3CLpro fragment. The 3CLpro activity was determined using the fluorogenic substrate DabcylKTSAVLQ↓SGFRKME(Edans)NH_2. This substrate contains two fluorescent dyes selected in such a way as to realize the effect of the Förster resonance energy transfer (FRET). The substrate hydrolysis results in the disappearance of the conditions required for FRET to occur, leading to an increase in the fluorescence intensity. The addition of potential inhibitors into the enzyme—substrate system makes it possible to evaluate the inhibitory activity on the basis of the change in the fluorescence increase rate. The IC_{50} value corresponds to the test compound concentration that reduces the fluorescence level by 50% of the value observed without an inhibitor. As reference compounds, we used well-known protease inhibitors ML188 and disulfiram,[18] the semi-inhibitory concentrations IC_{50} of which are 1.56±0.55 and 6.25±1.97 μmol L^{-1}, respectively.

All tested compounds, except for compound **1g** containing 1,4-dihydroindeno[1,2-*c*]pyrazole fragment, exhibited no activity. In the case of compound **1g**, the IC_{50} concentration was 100±5.7 μmol L^{-1}. It should be noted for comparison that symmetrically *N*,*N*′-disubstituted 1,5-dimethylbispidin-9-one containing two fragments of 1,4-dihydroindeno[1,2-*c*]-pyrazole, which, according to computer docking, covalently binds to the Cys145 amino acid residue of the main protease 3CLpro, has an IC_{50} concentration of 13.0±2.1 μmol L^{-1}.[11] It is noteworthy that for compound **1g**, which showed moderate activity against the main protease, the calculated binding energy was the highest among all considered bispidine derivatives.

In modern medicinal chemistry, publications on inactive compounds or compounds with low activity are controversial and may be considered not important,[19] while the compounds themselves may be regarded as irrelevant. However, data on these compounds are important for the development of computer-aided drug design methods,[20] which make it possible to build, optimize, and evaluate new chemical objects.

Thus, in this work, a series of non-symmetric amides of *N*-benzylbispidin-9-ol (eight of which have not been reported before) were synthesized, their molecular modelling was carried out, and their inhibitory activity against the main protease 3CLpro of the SARS-CoV-2 virus was studied. It is found that *N*-benzyl-*N*′-acylbispidin-9-ols exhibit no pronounced inhibitory activity in contrast to symmetric *N*,*N*′-disubstituted bispidinones. Nonetheless, it is shown that compound **1g** may be promising for subsequent modifications to obtain compounds with high inhibitory activity.

Experimental

NMR spectra were recorded on a Bruker Avance 400 spectrometer (operating frequencies are 400 MHz for ^1H and 101 MHz for ^{13}C) at 298 K using $SiMe_4$ as an internal standard. High resolution mass spectra (HRMS) using electrospray ionization (ESI) were recorded on a Bruker MicrOTOF II spectrometer. The course of reactions and the purity of the synthesized compounds were monitored

by TLC on the Merck TLC Silica gel 60G F254 plates. All used reagents and solvents (of 90.0—99.9% purity) were those commercially available (Sigma-Aldrich, ABCR, Acros Organics). If necessary, they were further purified to analytical purity by standard procedures immediately before use. Parent *N*-benzyl-1,5-dimethylbispidin-9-ol **2** and compound **1a** were prepared by known methods.[12] Acyl chlorides RC(O)Cl **3** (R = Me, Ph, C_4H_3S) were obtained from commercial sources, hydrochlorides of isonicotinoyl[21] and nicotinoyl[22] chlorides were synthesized using the corresponding methods, other acyl chlorides were prepared by the method reported previously.[11]

Synthesis of compounds 1b—h (general procedure). Corresponding acyl chloride **3** (1.9 mmol) and triethylamine (0.19 g, 0.27 mL, 1.9 mmol) were added to a suspension of *N*-benzyl-1,5-dimethylbispidin-9-ol (**2**) (0.495 g, 1.9 mmol) in dry acetonitrile (20 mL). The reaction mixture was stirred at room temperature for 6 h. The course of the reaction was monitored by TLC (using a $CHCl_3$—MeOH (5 : 1) mixture as an eluent). After completion of the reaction, the reaction mixture was poured into ice water (50 mL), the formed precipitate was filtered off and dried under reduced pressure in a vacuum desiccator over P_2O_5 to a constant sample weight.

1-(7-Benzyl-9-hydroxy-1,5-dimethyl-3,7-diazabicyclo[3.3.1]nonan-3-yl)ethan-1-one (1b). Colorless solid. Yield 0.333 g (58%). ^{1}H NMR (400 MHz, $CDCl_3$), δ: 0.87 (s, 3 H, CC$\underline{H}_3$); 0.92 (s, 3 H, CC$\underline{H}_3$); 1.98 (s, 3 H, NCOC$\underline{H}_3$); 2.27—2.33 (m, 2 H, H(8a)/H(6a)*, H(8e)/H(6e)); 2.37—2.48 (m, 3 H, H(6e)/H(8e), H(6a)/H(8a) + + O$\underline{H}$); 2.58 (d, 1 H, H(4a), *J* = 11.1 Hz); 2.96 (d, 1 H, H(2a), *J* = 13.4 Hz); 3.10 (d, 1 H, C$\underline{H}_2$Ph, *J* = 12.6 Hz); 3.22 (s, 1 H, C$\underline{H}$OH); 3.46—3.52 (m, 2 H, C$\underline{H}_2$Ph, H(2e)); 4.61 (d, 1 H, H(4e), *J* = 13.5 Hz); 7.18—7.33 (m, 5 H, Ph). ^{13}C NMR (101 MHz, $CDCl_3$), δ: 20.84 (C$\underline{C}$H$_3$), 20.91 (C$\underline{C}$H$_3$), 21.87 (NCO$\underline{C}$H$_3$), 35.71 (C(1)/C(5)), 36.09 (C(5)/C(1)), 51.53 (C(2)/C(4)/C(6)/C(8)), 56.55 (C(4)/C(2)/C(6)/C(8)), 56.63 (C(6)/C(2)/C(4)/C(8)), 57.77 (C(8)/C(2)/C(4)/C(6)), 62.90 (C$\underline{H}_2$Ph), 77.77 (C$\underline{C}$HOH), 126.64 (Ph), 127.73 (Ph), 128.88 (Ph), 138.11 (Ph), 168.71 (C=O). HRMS: *m*/*z* 303.2067 [M + H]$^+$. Calculated for $C_{18}H_{27}N_2O_2^+$: M = 303.2067.

(7-Benzyl-9-hydroxy-1,5-dimethyl-3,7-diazabicyclo[3.3.1]nonan-3-yl)(phenyl)methanone (1c). Colorless solid. Yield 0.478 g (69%). ^{1}H NMR (400 MHz, DMSO-d_6), δ: 0.62 (s, 3 H, CC$\underline{H}_3$); 0.77 (s, 3 H, CC$\underline{H}_3$); 2.12 (d, 1 H, H(6a)/H(8a), *J* = 10.7 Hz); 2.23—2.31 (m, 2 H, H(8a)/H(6a), H(8e)/H(6e)); 2.37 (d, 1 H, H(6e)/H(8e), *J* = 10.6 Hz); 2.65 (d, 1 H, H(4a), *J* = 13.4 Hz); 3.03 (d, 1 H, H(2a), *J* = 13.4 Hz); 3.11—3.16 (m, 2 H, C$\underline{H}$OH + C$\underline{H}_2$Ph); 3.42 (d, 1 H, C$\underline{H}_2$Ph, *J* = 13.3 Hz); 3.53 (d, 1 H, H(2e), *J* = 13.4 Hz); 4.48 (d, 1 H, H(4e), *J* = 13.4 Hz); 4.95 (s, 1 H, OH); 7.16—7.43 (m, 10 H, 2 Ph). ^{13}C NMR (101 MHz, DMSO-d_6), δ: 21.04 (C$\underline{C}$H$_3$), 21.43 (C$\underline{C}$H$_3$), 35.68 (C(1)/C(5)), 36.15 (C(5)/C(1)), 51.72 (C(2)/C(4)/C(6)/C(8)), 56.83 (C(4)/C(2)/C(6)/C(8)), 57.38 (C(6)/C(2)/C(4)/C(8)), 57.82 (C(8)/C(2)/C(4)/C(6)), 63.02 (C$\underline{H}_2$Ph), 75.53 (C$\underline{C}$HOH), 126.62 (Ph), 126.72 (Ph′), 128.15 (Ph′), 128.30 (Ph), 128.64 (Ph), 128.77 (Ph′), 137.36 (Ph′), 138.39 (Ph), 168.02 (C=O). HRMS: *m*/*z* 365.2229 [M + H]$^+$. Calculated for $C_{23}H_{29}N_2O_2^+$: 365.2224.

(7-Benzyl-9-hydroxy-1,5-dimethyl-3,7-diazabicyclo[3.3.1]nonan-3-yl)(thiophen-2-yl)methanone (1d). Colorless solid. Yield 0.465 g (66%). ^{1}H NMR (400 MHz, DMSO-d_6), δ: 0.70 (s, 3 H, CC$\underline{H}_3$); 0.78 (s, 3 H, CC$\underline{H}_3$); 2.15—2.24 (m, 3 H, H(6a)/H(8a), H(8a)/H(6a), H(8e)/H(6e)); 2.34 (d, 1 H, H(6e)/H(8e), *J* = 10.6 Hz); 2.67 (d, 1 H, H(4a), *J* = 13.4 Hz); 3.11—3.27 (m, 3 H, C$\underline{H}_2$Ph, C$\underline{H}$OH); 3.35 (d, 1 H, H(2a), *J* = 12.9 Hz); 3.90 (d, 1 H, H(2e), *J* = 13.2 Hz); 4.46 (d, 1 H, H(4e), *J* = 13.4 Hz); 4.96 (d, 1 H, O$\underline{H}$, *J* = 5.1 Hz); 7.06 (dd, 1 H, thiophene, *J* = 5.0 Hz, *J* = 3.6 Hz); 7.10—7.29 (m, 6 H, Ph + thiophene); 7.68 (d, 1 H, thiophene, *J* = 5.0 Hz). ^{13}C NMR (101 MHz, DMSO-d_6), δ: 21.10 (C$\underline{C}$H$_3$), 21.33 (C$\underline{C}$H$_3$), 35.81 (C(1)/C(5)), 36.26 (C(5)/C(1)), 52.34 (C(2)/C(4)/C(6)/C(8)), 57.14 (C(4)/C(2)/C(6)/C(8)), 57.47 (C(6)/C(2)/C(4)/C(8)), 57.52 (C(8)/C(2)/C(4)/C(6)), 62.95 (C$\underline{H}_2$Ph), 75.45 (C$\underline{C}$HOH), 126.64 (Ph), 126.79 (thiophene), 128.04 (thiophene), 128.30 (Ph), 128.51 (thiophene), 128.62 (Ph), 138.53 (Ph), 161.78 (C=O). HRMS: *m*/*z* 371.1798 [M + H]$^+$. Calculated for $C_{21}H_{27}N_2O_2S^+$: 371.1788.

(7-Benzyl-9-hydroxy-1,5-dimethyl-3,7-diazabicyclo[3.3.1]nonan-3-yl)(1-methyl-5-phenyl-1*H*-pyrazol-3-yl)methanone (1e). Colorless solid. Yield 0.678 g (80%). ^{1}H NMR (400 MHz, $CDCl_3$), δ: 0.90 (s, 3 H, CC$\underline{H}_3$); 0.98 (s, 3 H, CC$\underline{H}_3$); 2.28 (d, 1 H, H(6a)/H(8a), *J* = 11.2 Hz); 2.36—2.45 (m, 3 H, H(8a)/H(6a), H(8e)/H(6e), O$\underline{H}$); 2.62—2.69 (m, 2 H, H(4a), H(6e)/H(8e)); 3.09 (d, 1 H, H(2a), *J* = 13.6 Hz); 3.22 (d, 1 H, C$\underline{H}_2$Ph, *J* = 13.1 Hz); 3.29 (s, 1 H, C$\underline{H}$OH); 3.44 (d, 1 H, C$\underline{H}_2$Ph, *J* = 13.0 Hz); 3.85 (s, 3 H, NC$\underline{H}_3$); 4.65 (d, 1 H, H(2e), *J* = 13.6 Hz); 4.78 (d, 1 H, H(4e), *J* = 13.6 Hz); 6.69 (s, 1 H, Pyr); 7.10—7.31 (m, 5 H, Ph); 7.40—7.55 (m, 5 H, Ph). ^{13}C NMR (101 MHz, $CDCl_3$), δ: 21.04 (C$\underline{C}$H$_3$), 21.10 (C$\underline{C}$H$_3$), 35.95 (C(1)/C(5)), 36.27 (C(5)/C(1)), 37.47 (N$\underline{C}$H$_3$), 52.34 (C(2)/C(4)/C(6)/C(8)), 56.66 (C(4)/C(2)/C(6)/C(8)), 56.78 (C(6)/C(2)/C(4)/C(8)), 57.49 (C(8)/C(2)/C(4)/C(6)), 62.83 (C$\underline{H}_2$Ph), 78.31 (C$\underline{C}$HOH), 108.08 (Pyr), 126.30 (Ph), 127.60 (Ph), 128.35 (Ph + Ph′), 128.67 (Ph), 129.67 (Ph′), 138.12 (Ph), 143.54 (Pyr), 146.18 (Pyr), 162.54 (C=O). HRMS: *m*/*z* 445.2602 [M + H]$^+$. Calculated for $C_{27}H_{33}N_4O_2^+$: 445.2598.

(7-Benzyl-9-hydroxy-1,5-dimethyl-3,7-diazabicyclo[3.3.1]nonan-3-yl)(1-methyl-5-(thiophen-2-yl)-1*H*-pyrazol-3-yl)methanone (1f). Colorless solid. Yield 0.735 g

* Here and below, through a slash, atoms are indicated for which an exact assignment is impossible.

(86%). ^{1}H NMR (400 MHz, $CDCl_3$), δ: 0.89 (s, 3 H, CC$\underline{H}_3$); 0.98 (s, 3 H, CC$\underline{H}_3$); 2.20—2.48 (m, 4 H, H(6a)/H(8a), H(8a)/H(6a), H(8e)/H(6e), O$\underline{H}$); 2.62—2.68 (m, 2 H, H(4a), H(6e)/H(8e)); 3.08 (d, 1 H, H(2a), *J* = 13.7 Hz); 3.19 (d, 1 H, C$\underline{H}_2$Ph, *J* = 12.9 Hz); 3.28 (s, 1 H, C$\underline{H}$OH); 3.45 (d, 1 H, C$\underline{H}_2$Ph, *J* = 12.9 Hz); 3.92 (s, 3 H, NC$\underline{H}_3$); 4.64 (d, 1 H, H(2e), *J* = 13.6 Hz); 4.78 (d, 1 H, H(4e), *J* = 13.6 Hz); 6.79 (s, 1 H, Pyr); 7.11—7.26 (m, 7 H, Ph, thiophene); 7.44 (d, 1 H, thiophene, *J* = 5.0 Hz). ^{13}C NMR (101 MHz, $CDCl_3$), δ: 21.00 (2C$\underline{C}H_3$), 35.96 (C(1)/C(5)), 36.24 (C(5)/C(1)), 37.78 (N$\underline{C}H_3$), 52.37 (C(2)/C(4)/C(6)/C(8)), 56.52 (C(4)/C(2)/C(6)/C(8)), 56.73 (C(6)/C(2)/C(4)/C(8)), 57.55(C(8)/C(2)/C(4)/C(6)), 62.86 (C$\underline{H}_2$Ph), 78.17 (C$\underline{H}$OH), 108.91 (Pyr), 126.32 (Ph), 126.55 (Ph), 126.88 (Ph), 127.32 (thiophene), 127.58 (thiophene), 128.69 (thiophene), 130.17 (thiophene), 136.67 (Pyr), 138.04 (Ph), 146.19 (Pyr), 162.18 (C=O). HRMS: *m/z* 451.2163 $[M + H]^+$. Calculated for $C_{25}H_{31}N_4O_2S^+$: 451.2162.

(7-Benzyl-9-hydroxy-1,5-dimethyl-3,7-diazabicyclo-[3.3.1]nonan-3-yl)(1-methyl-1,4-dihydroindeno[1,2-*c*]-pyrazol-3-yl)methanone (1g). Colorless solid. Yield 0.659 g (76%). ^{1}H NMR (400 MHz, $CDCl_3$), δ: 0.91 (s, 3 H, CC$\underline{H}_3$); 0.99 (s, 3 H, CC$\underline{H}_3$); 2.21—2.48 (m, 4H, H(6a)/H(8a), H(8a)/H(6a), H(8e)/H(6e), O$\underline{H}$), 2.62—2.69 (m, 2 H, H(4a), H(6e)/H(8e)), 3.11 (d, 1 H, H(2a), *J* = 13.7 Hz); 3.19 (d, 1 H, C$\underline{H}_2$Ph, *J* = 13.0 Hz); 3.30 (s, 1 H, C$\underline{H}$OH); 3.43 (d, 1 H, C$\underline{H}_2$Ph, *J* = 13.1 Hz); 3.79 (d, 2 H, C$\underline{H}_2$, *J* = 5.0 Hz); 4.09 (s, 3 H, NC$\underline{H}_3$); 4.82 (d, 1 H, H(2e), *J* = 13.5 Hz); 5.03 (d, 1 H, H(4e), *J* = 13.6 Hz); 7.00—7.10 (m, 3 H, Ph); 7.18 (d, 2 H, Ph, *J* = 7.2 Hz); 7.26—7.30 (dd, 1 H, Ph, *J* = 7.4 Hz, *J* = 7.5 Hz); 7.37 (dd, 1 H, Ph, *J* = 7.4 Hz, *J* = 7.5 Hz); 7.52—7.56 (m, 2 H, Ph). ^{13}C NMR (101 MHz, $CDCl_3$), δ: 21.06 (2C$\underline{C}H_3$), 29.79 (CH_2), 36.01 (C(1)/C(5)), 36.28 (C(5)/C(1)), 37.71 (N$\underline{C}H_3$), 52.39 (C(2)/C(4)/C(6)/C(8)), 56.40 (C(4)/C(2)/C(6)/C(8)), 56.61 (C(6)/C(2)/C(4)/C(8)), 57.44 (C(8)/C(2)/C(4)/C(6)), 62.76 (C$\underline{H}_2$Ph), 78.25 (C$\underline{H}$OH), 117.87 (Pyr), 125.91 (Ph′), 126.09 (Ph′), 126.21 (Ph′), 126.30 (Ph), 127.42 (Ph), 128.45 (Ph), 129.33 (Ph′), 131.27 (Ph′), 138.13 (Ph), 140.62 (Pyr), 148.71 (Ph′), 148.97 (Pyr), 162.04 (C=O). HRMS: *m/z* 457.2596 $[M + H]^+$. Calculated for $C_{28}H_{33}N_4O_2^+$: 457.2598.

(7-Benzyl-9-hydroxy-1,5-dimethyl-3,7-diazabicyclo-[3.3.1]nonan-3-yl)(1-methyl-4,5-dihydro-1*H*-benzo[g]-indazol-3-yl)methanone (1h). Colorless solid. Yield 0.715 g (80%). ^{1}H NMR (400 MHz, $CDCl_3$), δ: 0.90 (s, 3 H, CC$\underline{H}_3$); 0.98 (s, 3 H, CC$\underline{H}_3$); 2.31 (d, 1 H, H(6a)/H(8a), *J* = 11.3 Hz); 2.35 (d, 2 H, H(8e)/H(6e), O$\underline{H}$, *J* = 11.5 Hz); 2.43 (d, 1 H, H(8a)/H(6a), *J* = 11.2 Hz); 2.58—2.67 (m, 2 H, H(4a), H(6e)/H(8e)); 2.82—3.15 (m, 5 H, H(2a), 2 C$\underline{H}_2$); 3.26 (s, 1 H, C$\underline{H}$OH); 3.30 (d, 1 H, C$\underline{H}_2$Ph, *J* = 13.2 Hz); 3.38 (d, 1 H, C$\underline{H}_2$Ph, *J* = 13.1 Hz); 4.12 (s, 3 H, C$\underline{H}_3$); 4.60 (d, 1 H, H(2e), *J* = 13.5 Hz); 4.76 (d, 1 H, H(4e), *J* = 13.5 Hz); 7.09—7.40 (m, 8 H, Ph); 7.58 (d 1 H, Ph, *J* = 7.7 Hz). ^{13}C NMR (101 MHz, $CDCl_3$), δ: 19.61 (CH_2), 21.19 (C$\underline{C}H_3$), 21.29 (C$\underline{C}H_3$), 30.25 (CH_2′), 35.91 (C(1)/C(5)), 36.29 (C(5)/C(1)), 39.42 (N$\underline{C}H_3$), 52.16 (C(2)/C(4)/C(6)/C(8)), 56.73 (C(4)/C(2)/C(6)/C(8)), 56.93 (C(6)/C(2)/C(4)/C(8)), 57.23 (C(8)/C(2)/C(4)/C(6)), 62.64 (C$\underline{H}_2$Ph), 78.40 (C$\underline{H}$OH), 120.31 (Pyr), 121.63 (Ph′), 126.27 (Ph′), 126.34 (Ph′), 126.58 (Ph), 127.30 (Ph′), 127.60 (Ph), 128.50 (Ph′), 128.61 (Ph), 137.42 (Pyr), 137.94 (Ph′), 138.11 (Ph), 141.40 (Pyr), 162.88 (C=O). HRMS: *m/z* 471.2756 $[M + H]^+$. Calculated for $C_{29}H_{35}N_4O_2^+$: 471.2755.

Synthesis of compounds 1i and 1j (general procedure). Hydrochloride of isonicotinoyl chloride (in the case of **1i**) or nicotinoyl chloride (in the case of **1j**) in the amount of 1.9 mmol and triethylamine (0.39 g, 0.53 mL, 3.8 mmol) were added to a suspension of benzylbispidinol (**2**) (0.495 g, 1.9 mmol) indry acetonitrile (20 mL). The reaction mixture was stirred at room temperature for 6 h. The completion of the reaction was checked by TLC (using a $CHCl_3$—MeOH (5 : 1) mixture as an eluent). Then, the reaction mixture was poured into ice water (50 mL). The formed precipitate was filtered off and dried under reduced pressure in a vacuum desiccator over P_2O_5 to a constant sample weight.

(7-Benzyl-9-hydroxy-1,5-dimethyl-3,7-diazabicyclo-[3.3.1]nonan-3-yl)(pyridin-4-yl)methanone (1i). Colorless solid. Yield 0.329 g (50%). ^{1}H NMR (400 MHz, $CDCl_3$), δ: 0.80 (s, 3 H, CC$\underline{H}_3$); 0.94 (s, 3 H, CCH_3); 2.25—2.33 (m, 2 H, H(6a)/H(8a), O$\underline{H}$); 2.37—2.44 (m, 2 H, H(8a)/H(6a), H(8e)/H(6e)); 2.65 (d, 1 H, H(6e)/H(8e), *J* = 11.2 Hz); 2.70 (dd, 1 H, H(4a), *J* = 13.7 Hz, *J* = 2.2 Hz); 2.97 (d, 1 H, H(2a), *J* = 13.5 Hz); 3.27 (s, 1 H, C$\underline{H}$OH); 3.32 (d, 1 H, C$\underline{H}_2$Ph, *J* = 13.2 Hz); 3.42 (dd, 1 H, H(2e), *J* = 13.4 Hz, *J* = 2.1 Hz); 3.54 (d, 1 H, C$\underline{H}_2$Ph, *J* = 13.2 Hz); 4.71 (dd, 1 H, H(4e), *J* = 13.7 Hz, *J* = 2.1 Hz); 7.13—7.19 (m, 2 H, Py); 7.24—7.43 (m, 5 H, Ph); 8.58 (d, 2 H, Py, *J* = 5.4 Hz). ^{13}C NMR (101 MHz, $CDCl_3$), δ: 20.67 (C$\underline{C}H_3$), 20.87 (C$\underline{C}H_3$), 35.70 (C(1)/C(5)), 36.18 (C(5)/C(1)), 51.78 (C(2)/C(4)/C(6)/C(8)), 56.73 (C(4)/C(2)/C(6)/C(8)), 57.33 (C(6)/C(2)/C(4)/C(8), C(8)/C(2)/C(4)/C(6)), 63.14 (C$\underline{H}_2$Ph), 77.21 (C$\underline{H}$OH), 120.85 (Py), 126.73 (Ph), 128.06 (Ph), 128.72 (Ph), 137.42 (Ph), 144.34 (Py), 149.60 (Py), 166.49 (C=O). HRMS: *m/z* 366.2185 $[M + H]^+$. Calculated for $C_{22}H_{28}N_3O_2^+$: 366.2176.

(7-Benzyl-9-hydroxy-1,5-dimethyl-3,7-diazabicyclo-[3.3.1]nonan-3-yl)(pyridin-3-yl)methanone (1j). Colorless solid. Yield 0.375 g (54%). ^{1}H NMR (400 MHz, $CDCl_3$), δ: 0.79 (s, 3 H, CC$\underline{H}_3$); 0.93 (s, 3 H, CC$\underline{H}_3$); 2.28 (dd, 1 H, H(6a)/H(8a), *J* = 11.3 Hz, *J* = 2.3 Hz); 2.34—2.44 (m, 2 H, H(8a)/H(6a), H(8e)/H(6e)); 2.47—2.59 (m, 1 H, O$\underline{H}$); 2.64 (d, 1 H, H(6e)/H(8e), *J* = 11.2 Hz); 2.71 (dd, 1 H, H(4a), *J* = 13.7 Hz, *J* = 2.2 Hz); 3.02 (dd, 1 H, H(2a), *J* = 13.4 Hz, *J* = 1.9 Hz); 3.26 (s, 1 H, C$\underline{H}$OH); 3.30 (d, 1 H, C$\underline{H}_2$Ph, *J* = 13.2 Hz); 3.48—3.56 (m, 2 H, C$\underline{H}_2$Ph,

H(2e)); 4.72 (dd, 1 H, H(4e), J = 13.7 Hz, J = 2.1 Hz); 7.18—7.37 (m, 6 H, Ph, Py), 7.63 (dt, 1 H, py, J = 7.8 Hz, J = 1.9 Hz); 8.59—8.61 (m, 2 H, Py). ^{13}C NMR (101 MHz, $CDCl_3$), δ: 20.71 ($C\underline{C}H_3$), 20.89 ($C\underline{C}H_3$), 35.68 (C(1)/C(5)), 36.23 (C(5)/C(1)), 51.99 (C(2)/C(4)/C(6)/C(8)), 56.66 (C(4)/C(2)/C(6)/C(8)), 57.35 (C(6)/C(2)/C(4)/C(8)), 57.75 (C(8)/C(2)/C(4)/C(6)), 63.03 ($\underline{C}H_2Ph$), 77.43 (<u>C</u>HOH), 123.05 (Py), 126.65 (Ph), 127.99 (Ph), 128.54 (Ph), 132.38 (Py), 134.48 (Py), 137.45 (Ph), 147.37 (Py), 149.65 (Py), 166.59 (C=O). HRMS: m/z 366.2180 $[M + H]^+$. Calculated for $C_{22}H_{28}N_3O_2^+$: 366.2176.

Molecular modelling. Molecular modeling was carried out in the Schrodinger Maestro visualization environment using applications from the Schrödinger Small Molecule Drug Discovery Suite 2016-1 program package (Schrödinger, LLC, 2016). The 3D structures of the derivatives were obtained empirically in the LigPrep application using the OPLS3 force field.[23] All possible tautomeric forms of compounds and various states of polar protons of molecules at pH 7.0±2.0 were taken into account. The X-ray diffraction model of the main protease of SARS-CoV-2 (PDB ID 7L0D) was used in the calculations.[16] Modeling of the possible mechanism of non-covalent inhibition of the main protease was performed by molecular docking of compounds to the binding site of the ML188 inhibitor using the Glide application.[24] The search area for the scoring function was selected automatically based on the size and physicochemical properties of the ML188 inhibitor. The XP (Extra Precision) algorithm of increased docking accuracy was used. Docking was performed using the score in place mode, *i.e.*, in comparison with the calculation of the scoring function for the ML188 inhibitor in the coordinates of the X-ray diffraction model. Non-covalent interactions of compounds at the binding site were visualized using the Biovia Discovery Studio Visualizer program (v.17.2, San Diego: Dassault Systèmes, 2016).

Measurement of inhibitory activity against the viral protease. The 3CLpro activity was measured using the fluorogenic substrate DabcylKTSAVLQ↓SGFRKME(Edans) NH_2 on a CLARIOstar Plus microplate reader (BMG Labtech, Germany) with the use of wavelengths of 355 and 460 nm for excitation and detection, respectively. The reaction mixtures were prepared in a 384-well plate, incubated for 30 min; the measurements were carried out at 30 °C. Each well contained one reaction mixture consisting of Tris HCl buffer (pH 7.3, 20 mmol of tris(hydroxymethyl)aminomethane), NaCl (100 mmol), EDTA (1 mmol), DTT (dithiotreitol, 1 mmol)), substrate (10 μmol), an inhibitor (400 μmol), and 3CLpro ($3 \cdot 10^{-7}$ mol). The instrument was calibrated using a peptide solution subjected to complete hydrolysis. The fluorescence value of this mixture was taken as 80%. The measurements were carried out in the kinetic scan mode (50 cycle of 10 s). All experiments were repeated three times (n = 3). Calculations were performed using the accompanying MARS Data Analysis software (BMG LABTECH, Germany). The IC_{50} value corresponded to the test compound concentration that reduced the fluorescence level by 50% of the value observed without an inhibitor.

This work was performed under financial support of the Russian Foundation for Basic Research (Project No. 20-04-60215). Biological testing was carried out under financial support of Ministry of Science and Higher Education of the Russian Federation (Agreement No. 075-15-2021-1355 dated 12.10.2021) as part of the implementation of certain activities of the Federal Scientific and Technical Program for the Development of Synchrotron and Neutron Research and Research Infrastructure for 2019—2027.

The authors express their gratitude to the Information and Computing Center of Novosibirsk State University for the provided computing resources.

No human or animal subjects were used in this research.

The authors declare no competing interests.

References

1. I. Tomassoli, D. Gündisch, *Curr. Top. Med. Chem.*, 2016, **16**, 1314—1342; DOI: 10.2174/1568026615666150915111434.
2. A. V. Medved´ko, A. I. Dalinger, V. N. Nuriev, V. S. Semashko, A. V. Filatov, A. A. Ezhov, A. V. Churakov, J. A. K. Howard, A. A. Shiryaev, A. E. Baranchikov, V. K. Ivanov, S. Z. Vatsadze, *Nanomaterials*, 2019, **9**, 89—106; DOI: 10.3390/nano9010089.
3. A. I. Dalinger, A. V. Medved´ko, M. A. Kalinin, V. A. Sereda, A. V. Churakov, S. Z. Vatsadze, *Russ. Chem. Bull.*, 2021, **70**, 1002—1005; DOI: 10.1007/s11172-021-3180-9.
4. M. A. Kalinin, S. M. Antropov, A. V. Medvedko, A. O. Gudovannyy, K. A. Lyssenko, S. Z. Vatsadze, *Russ. Chem. Bull.*, 2021, **70**, 2247—2251; DOI: 10.1007/s11172-021-3341-x.
5. N. S. Zefirov, V. A. Palyulin, in *Topics In Stereochemestry*, vol. 20, Eds E. L. Eliel, S. H. Wilen, John Wiley & Sons, Inc., 1991, p. 171.
6. P. Comba, M. Kerscher, W. Schiek, *Progr. Inorg. Chem.*, 2007, **55**, 613—704; DOI: 10.1002/9780470144428.ch9.
7. A. V. Medved´ko, B. V. Egorova, A. A. Komarova, R. D. Rakhimov, D. P. Krut´ko, S. N. Kalmykov, S. Z. Vatsadze, *ACS Omega*, 2016, **1**, 854—867; DOI: 10.1021/acsomega.6b00237.
8. K. V. Kudryavtsev, D. A. Shulga, V. I. Chupakhin, E. I. Sinauridze, F. I. Ataullakhanov, S. Z. Vatsadze,

Tetrahedron, 2014, **70**, 7854—7864; DOI: 10.1016/j.tet.2014.09.009.
9. S. Z. Vatsadze, D. A. Shulga, Y. D. Loginova, I. A. Vatsadze, L. Yu, H. Wang, K. V. Kudryavtsev, *Mendeleev Commun*., 2016, **26**, 212—213; DOI: 10.1016/j.mencom.2016.04.011.
10. V. Haridas, K. S. Rajgokul, S. Sadanandan, T. Agrawal, V. Sharvani, M. V. S. Gopalakrishna, M. B. Bijesh, K. L. Kumawat, A. Basu, G. R. Medigeshi, *PLoS Negl. Trop. Dis.*, 2013, **7**, e2005; DOI: 10.1371/journal.pntd.0002005.
11. D. Shcherbakov, D. Baev, M. Kalinin, A. Dalinger, V. Chirkova, S. Belenkaya, A. Khvostov, D. Krut´ko, A. Medved´ko, E. Volosnikova, E. Sharlaeva, D. Shanshin, T. Tolstikova, O. Yarovaya, R. Maksyutov, N. Salakhutdinov, S. Vatsadze, *ACS Med. Chem. Lett*, 2022, **13**, 140—147; DOI: 10.1021/acsmedchemlett.1c00299.
12. S. Z. Vatsadze, V. S. Tyurin, A. I. Zatsman, M. A. Manaenkova, V. S. Semashko, D. P. Krut´ko, N. V. Zyk, A. V. Churakov, L. G. Kuz´mina, *Russ. J. Org. Chem.*, 2006, **42**, 1225—1231; DOI: 10.1134/S1070428006080215.
13. S. Günther, P. Y. A. Reinke, Y. Fernández-García, J. Lieske, T. J. Lane, H. M. Ginn, F. H. M. Koua, C. Ehrt, W. Ewert, D. Oberthuer, O. Yefanov, S. Meier, K. Lorenzen, B. Krichel, J.-D. Kopicki, L. Gelisio, W. Brehm, I. Dunkel, B. Seychell, H. Giesler, B. Norton-Baker, B. Escudero-Pérez, M. Domaracky, S. Saouane, A. Tolstikova, T.A. White, A. Hänle, M. Groessler, H. Fleckenstein, F. Trost, M. Galchenkova, Y. Gevorkov, C. Li, S. Awel, A. Peck, M. Barthelmess, F. Schluenzen, P. Lourdu Xavier, N. Werner, H. Andaleeb, N. Ullah, S. Falke, V. Srinivasan, B. A. França, M. Schwinzer, H. Brognaro, C. Rogers, D. Melo, J.J. Zaitseva-Doyle, J. Knoska, G.E. Peña-Murillo, A.R. Mashhour, V. Hennicke, P. Fischer, J. Hakanpää, J. Meyer, P. Gribbon, B. Ellinger, M. Kuzikov, M. Wolf, A. R. Beccari, G. Bourenkov, D. von Stetten, G. Pompidor, I. Bento, S. Panneerselvam, I. Karpics, T. R. Schneider, M. M. Garcia-Alai, S. Niebling, C. Günther, C. Schmidt, R. Schubert, H. Han, J. Boger, D.C.F. Monteiro, L. Zhang, X. Sun, J. Pletzer-Zelgert, J. Wollenhaupt, C. G. Feiler, M. S. Weiss, E.-C. Schulz, P. Mehrabi, K. Karničar, A. Usenik, J. Loboda, H. Tidow, A. Chari, R. Hilgenfeld, C. Uetrecht, R. Cox, A. Zaliani, T. Beck, M. Rarey, S. Günther, D. Turk, W. Hinrichs, H. N. Chapman, A. R. Pearson, C. Betzel, A. Meents, *Science*, 2021, **372**, 642—646; DOI: 10.1126/science.abf7945.
14. N. Drayman, J. K. DeMarco, K. A. Jones, S. A. Azizi, H. M. Froggatt, K.Tan, N. I. Maltseva, S. Chen, V. Nicolaescu, S. Dvorkin, K. Furlong, R. S. Kathayat, M. R. Firpo, V. Mastrodomenico, E. A. Bruce, M. M. Schmidt, R. Jedrzejczak, M. Á. Muñoz-Alía, B. Schuster, V. Nair, K. Han, A. O´Brien, A. Tomatsidou, B. Meyer, M. Vignuzzi, D. Missiakas, J. W. Botten, C. B. Brooke, H. Lee, S. C. Baker, B. C. Mounce, N. S. Heaton, W. E. Severson, K. E. Palmer, B. C. Dickinson, A. Joachimiak, G. Randall, S. Tay, *Science*, 2021, **373**, 931—936; DOI: 10.1126/science.abg5827.
15. A. Clyde, S. Galanie, D. W. Kneller, H. Ma, Y. Babuji, B. Blaiszik, A. Brace, T. Brettin, K. Chard, R. Chard, L. Coates, I. Foster, D. Hauner, V. Kertesz, N. Kumar, H. Lee, Z. Li, A. Merzky, J.G. Schmidt, L. Tan, M. Titov, A. Trifan, M. Turilli, H. Van Dam, S. C. Chennubhotla, S. Jha, A. Kovalevsky, A. Ramanathan, M. S. Head, R. Stevens, *J. Chem. Inf. Model.*, 2022, **62**, 116—128; DOI: 10.1021/acs.jcim.1c00851.
16. G. J. Lockbaum, A. C. Reyes, J. M. Lee, R. Tilvawala, E. A. Nalivaika, A. Ali, N. Kurt Yilmaz, P. R. Thompson, C. A. Schiffer, *Viruses*, 2021, **13**, 174; DOI: 10.3390/v13020174.
17. C. H. Zhang, E. A. Stone, M. Deshmukh, J. A. Ippolito, M. M. Ghahremanpour, J. Tirado-Rives, K. A. Spasov, S. Zhang, Y. Takeo, S. N. Kudalkar, Z. Liang, F. Isaacs, B. Lindenbach, S. J. Miller, K. S. Anderson, W. L. Jorgensen, *ACS Cent. Sci.*, 2021, **7**, 467—475; DOI: 10.1021/acscentsci.1c00039.
18. C. Ma, Y. Hu, J. A. Townsend, P. I. Lagarias, M. T. Marty, A. Kolocouris, J. Wang, *ACS Pharmacol. Transl. Sci.*, 2020, **3**, 1265—1277; DOI: 10.1021/acsptsci.0c00130.
19. E. López-López, E. Fernández-de Gortari, J. L. Medina-Franco, *Drug Discov. Today*, 2022, **27**, 2353—2362; DOI: 10.1016/j.drudis.2022.05.005.
20. J. J. Irwin, *J. Comput. Aided. Mol. Des.*, 2008, **22**, 193—199; DOI: 10.1007/s10822-008-9189-4.
21. O. Bagheri, H. Dehghani, M. Afrooz, *RSC Adv.*, 2015, **5**, 86191—86198; DOI: 10.1039/C5RA15894J.
22. C. Yang, A. R. Teixeira, Y. Shi, S. C. Born, H. Lin, Y. Li Song, B. Martin, B. Schenkel, M. Peer Lachegurabi, K. F. Jensen, *Green Chem.*, 2018, **20**, 886—893; DOI: 10.1039/C7GC03469E.
23. E. Harder, W. Damm, J. Maple, C. Wu, M. Reboul, J. Y. Xiang, L.Wang, D. Lupyan, M. K. Dahlgren, J. L. Knight, J. W. Kaus, D. S. Cerutti, G. Krilov, W. L. Jorgensen, R. Abel, R. A. Friesner, *J. Chem. Theory Comput.*, 2016, **12**, 281—296; DOI: 10.1021/acs.jctc.5b00864.
24. R. A. Friesner, R. B. Murphy, M. P. Repasky, L. L. Frye, J. R. Greenwood, T. A. Halgren, P. C. Sanschagrin, D. T. Mainz, *J. Med. Chem.*, 2006, **49**, 6177—6196; DOI: 10.1021/jm051256o.

Received May 25, 2022;
in revised form June 17, 2022;
accepted June 20, 2022